The Eurasia Proceedings of Science, Technology, Engineering & Mathematics (EPSTEM)
ISSN: 2602-3199

The Eurasia Proceedings of Science, Technology, Engineering & Mathematics (EPSTEM), 2023

Volume 23, Pages 100-105

ICRETS 2023: International Conference on Research in Engineering, Technology and Science

Green Hydrogen from PV-Supplied Sono-Electrolysis: Modelling and Experimental Investigations of the Mechanism and Performance

Nour Hane Merabet
Karlsruhe University of Applied Sciences

Kaouther Kerboua
National Higher School of Technology and Engineering

Abstract: Water and energy are the two most essential assets for a sustainable global human society. However, the high carbon footprint and global warming effects caused by non-renewable sources have made energy transition a key element to ensure sustainable development. Currently, hydrogen produced from water supplied by renewable energy is considered an ideal and sustainable energy carrier for the future. Herein, we investigate experimentally and theoretically using MatLab modeling the production of hydrogen via PV supplied alkaline electrolysis of water coupled to 40 kHz ultrasonic bath. Nickel plates and nickel foam were used as electrode's material immerged in 25% of KOH electrolyte while a 12V solar panel was used as a green source of power supply. The experimental and the modeling results related to the ultrasounds effect on hydrogen production efficiency showed a high agreement. The integration of ultrasound showed a reduction in electrode coverage by bubbles of approximately 54.8%, which was equivalent to 9.32% of the reduction in cell voltage according to the experiments.

Keywords: Sonoelectrolysis, Green hydrogen, Solar hydrogen, Ultrasound, Electrode coverage, Resistance.

Introduction

As the intergovernmental panel climate change's IPCC's latest report makes clear, while the temperature continues to rise, the risk of catastrophic events increases. Therefore, the transition to cleaner sources of energy is seen as an imperative step in order to reduce the carbon footprint of fossil fuels and conventional sources of energy (Hofrichter et al., 2022). Strategies for producing hydrogen that rely on renewable energy sources have been developed and implemented. Where the dispersion of ozone-depleting substances is also prohibited in these strategies (Gopinath & Marimuthu, 2022). In previous studies, the modelling and dimensioning of plants with hydrogen production from renewable energy sources such as PV have been investigated (Maurer et al., 2022).

The various established methods of solar hydrogen production use water as the critical reactant, as water separation produces oxygen and hydrogen (Burton et al., 2020). In addition, hydrogen production from water electrolysis is seen as a promising technology to produce hydrogen with high purity of 99.99% (Kerboua & Merabet, 2023).. Membrane free electrolyzers, with potential advantages in durability and manufacturability made possible by eliminating membranes or diaphragms from the device architecture, offer an attractive approach to reducing the cost of hydrogen (H2) production from water electrolysis (Pang et al., 2020). With easier device designs that can be made from fewer components, membraneless electrolysers have the potential to reduce material and assembly costs (Esposito, 2017). However, the increase of the ohmic resistance in the electrolyte remains a challenge for the electrolytic technique, as bubble formation limits the operating current density in alkaline water electrolysis, increases electrolyte resistance and reduces electrode active area (Marini et al., 2012).

It has been reported in literature that the integration of ultrasonic power has an improvement effect on mass transport enhancement due to the combined effect of microjets and microstreaming (Islam et al., 2020) and the efficient bubble removal from the electrode's surface (Li et al., 2009; Walton et al., 1996; Zadeh, 2014). In this context, it has been demonstrated very recently using modeling that the ohmic resistance and bubble coverage may be reduced due to the shockwave and microjets phenomena related to the ultrasound propagation in the electrolyte medium (Kerboua & Merabet, 2023).

The aim of the present study is to investigate experimentally and numerically the effect of ultrasound on the removal of bubbles from the electrode surface and to quantify the ultrasound effect on the fraction of the electrodes' area covered by bubbles, and hence the bubble and ohmic resistances, under a source of current, namely a PV solar panel as a source supplying a membraneless KOH electrolyzer.

Material and methods

Membraneless Sono-Electrolyzer

An H-cell electrolyzer of 300 mL of total capacity was filled with 25% of KOH aqueous solution. The electrolyzer counts nickel plates or nickel foam electrode's material of 13.5 cm^2 of working area. As a source of indirect continuous sonication, an ultrasound bath of 40 kHz and 60W_e has been employed.

Pv Solar Supply

The power supply consists of a 30 W monocrystalline solar photovoltaic panel (ET Solar-ET- M53640) connected to a Maximum Power Point Tracking regulator MPPT.

MatLab Modeling

The MatLab code is first based on the mathematical modeling of the PV supply, delivering a current I according to Eq.1 (Rahim et al., 2015; Villalva et al., 2009)

$$I = I_{pv} - I_d - I_{sh} \tag{1}$$

$$I_{pv} = \frac{\left(I_{pv0} + K\Delta T\right) G}{G_0} \tag{2}$$

$$I_d = I_0 \left(e^{\left(\frac{R_s I + V}{V_t . a}\right)} - 1 \right) \tag{3}$$

$$I_{sh} = \frac{V + R_s I}{R_p} \tag{4}$$

Where I_{pv} is the light-generated current of the PV cell is directly dependent on the solar irradiation G. As a next step, the produced current is injected to the electrolyser's mathematical model, accounting for Eqs.5 to 9 (Abul Kalam Azad & Khan, n.d.; Mohamed et al., 2016; Tijani et al., 2018).

$$U_{cell} = E_{rev} + U_{act} + U_{Ohm} + U_{Conc} \tag{5}$$

$$E_{rev}(T,P) = E_{rev}(T) + \frac{RT}{ZF} \ln\left(\frac{{P_v}^* (\mathrm{P} - P_v)^{1.5}}{P_v}\right) \tag{6}$$

$$U_{act} = \frac{2.3026\, RT}{ZF a_a} \log\left(\frac{I_a}{I_{0a}}\right) + \frac{2.3026\, RT}{ZF a_c} \log\left(\frac{I_c}{I_{0c}}\right) \tag{7}$$

$$U_{ohm} = I(R_{cell} + R_{electrodes} + R_{electrolyte} + R_{electrical}) \quad (8)$$

$$U_{conc} = \frac{RT}{ZF}\left(\ln\left(1 - \left(\frac{I}{I_{\lim}}\right)\right)\right) \quad (9)$$

Where E_{rev} is the reversible voltage, U_{act} is the activation voltage, U_{ohm} is the ohmic voltage and U_{conc} is the concentration voltage.

The effect of sonication was evaluated according to the electrode coverage by bubbles that govern the ohmic resistance as shown in Eqs.10 to 12 (Gambou et al., 2022).

$$R_{electrolyte} = R_{bf} + R_b \quad (10)$$

$$R_{bf} = \frac{1}{\sigma_{bf}}\left(\frac{d_a}{S_a} + \frac{d_c}{S_c}\right) \quad (11)$$

$$R_b = R_{bf}\left(\frac{1}{\left(1 - \frac{2}{3}e\right)^{1.5}} - 1\right) \quad (12)$$

S_a and S_c are anode and cathode cross sections respectively, d_a and d_c are distances from anode and cathode to membrane, σ_{bf} is the bubble-free electrolyte conductivity.

Results and Discussion

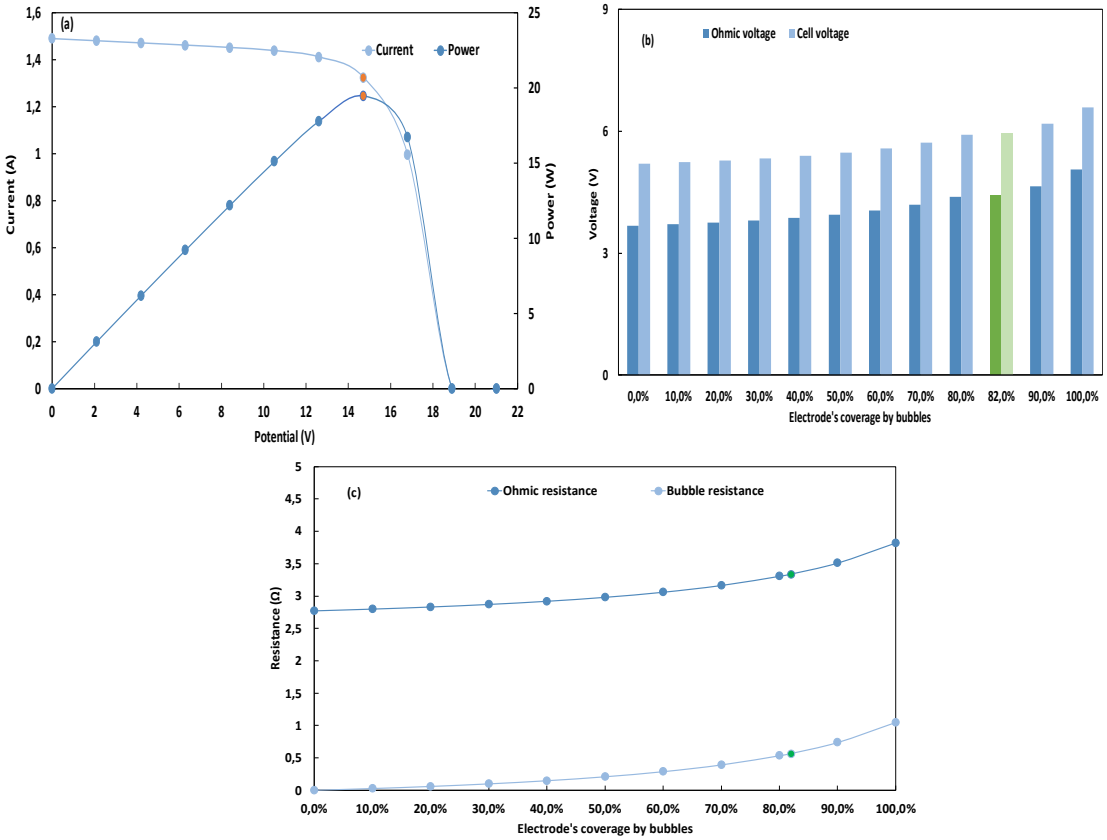

Figure 1. Simulated I-V and P-V characteristics of the solar panel feeding the electrolyzer under real solar radiation (a) and the effect of the electrodes' coverage by bubbles on the ohmic and cell voltage (b) and ohmic and bubble resistance (c) in silent conditions

Figure.1 presents the results of simulation under silent conditions and a solar irradiation of 827 W/m^2. Based on the polarization curve of the panel controlled by an MPPT controller, the performance of the PV panel is first described in Fig.1 (a) where the numerically obtained current-voltage I-V and power-potential P-V curves are described both with the maximum power point and its equivalent current and potential. Maximum power delivered corresponds to 19,481W, corresponding to a voltage of 14,7V and a current of 1,325A. Use of MPPTs allows to maintain input current at a steady value during electrolysis, avoiding any effect of intermittent photovoltaic power.

Both the obtained ohmic overpotential and the electrolysis potential depend on the percentage of electrode coverage, as shown in Fig.1 (b), it can be observed that, when the percentage of electrode coverage varies between 0 and 100%, the electrolysis cell studied develops a total potential ranging from 5.2386 to 6.5946 V (with an increase of 25.88%). The ohmic overpotential rises as well, with the above-mentioned variation of the e factor, from 3.6728 to 5.0650 V, which corresponds to 68.93% to 76.81% of the value of the total potential. According to the experimental resulting voltage that consist of cell potential of 5.9571 V, To meet the corresponding electrode coverage equals 81.98% and is represented in green color in Fig.1 (b). Accordingly, the ohmic overpotential characterizing the studied configuration is 4.4275V.

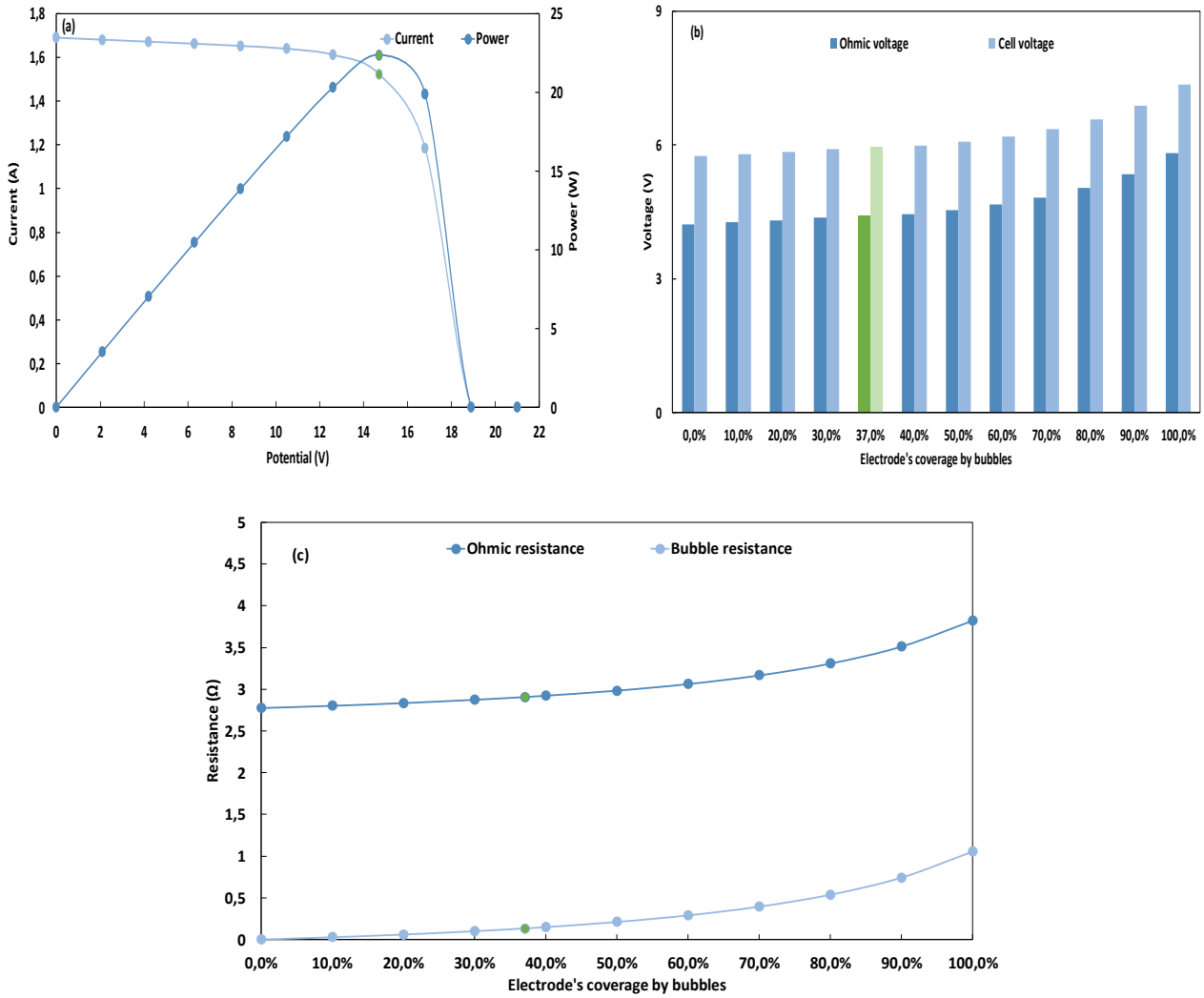

Figure 2. Simulated I-V and P-V characteristics of the solar panel feeding the electrolyzer under real solar radiation (a) and the effect of the electrodes' coverage by bubbles on the ohmic and cell voltage (b) and ohmic and bubble resistance (c) under ultrasonic power

The variation of the ohmic and bubble resistances in function of the electrode's bubble coverage is elucidated more specifically in Fig.1 (c), the variation of the e factor from 0 to 100% increases the Ohmic resistance from its lowest value of 2.7714 Ω to 3.822 Ω. In addition, the bubble resistance that constitutes 27.49% of the Ohmic resistance reaches its maximum value of 1.0505 Ω at a 100% of coverage consequence, the same cell potential as that retrieved experimentally with the silent configuration under a lower incident radiation and a higher

current were recorded. From Fig.2(a), it is clear that the maximum power equals 22.39 W and is achieved at a panel current of 1.523 A and a deliverable potential of 14.7 V. Thus, with the MPPT regulation, the electrolyzer is supplied with a direct current of 1.523 A.

Fig.2(b) presents the evolutions of the overall cell voltage and the Ohmic overpotential as a function of the electrodes' coverage percentage under the continuous ultrasound conditions. When the e factor is increased from 0 to 100%, the cell potential increases from 5.7558V to 7.3559V. The ohmic overpotential constitutes the major part of the cell potential, with a proportion ranging between 73.34% and 79.14%. while Experimental cell potentials measured under continuous sonication conditions were obtained for an electrode coverage of 30 to 40 %.

The simulation with a linear step on the value of *e* allowed the determination of the percentage of electrode coverage corresponding to the measured cell potential, i.e. 5.9577 V. This value corresponds to 37%, its associated ohmic overpotential is 4.4232 V, which corresponds to 2.904 Ω. In this case, as shown in Fig.7 (b), the bubble resistance is limited to 132.54mΩ, whereas it reaches 1.0505mΩ with 100% electrode coverage.

Conclusion

The effect of sonication on the bubble resistance and hence the ohmic resistance in a membraneless H-cell alkaline electrolyzer fed by PV has been studied experimentally and numerically in the present study. The combined experimental and fundamental modelling approach was based on the variation of the ohmic resistance parameters as a function of the coverage of the electrodes by bubbles, which was assumed to be reduced in the presence of sonication due to streaming, microjets and shockwavs.

The lowest electrode coverage was achieved with indirect continuous sonoelectrolysis, with a value of 37%, compared to 82% under silent conditions which corresponds to a reduction of approximately 54.8%. The resulting bubble resistance ranged from 569.81 mΩ in the absence of ultrasound to 132.54 mΩ with integrated continuous sonication. In fact, it is assumed that ultrasound results in a stirring effect in the bulk electrolyte and near the surface of the electrode, promoting the desorption of gas bubbles from the electrode.

Scientific Ethics Declaration

The authors declare that the scientific ethical and legal responsibility of this article published in EPSTEM journal belongs to the authors.

Acknowledgements or Notes

This article was presented as an oral presentation at the International Conference on Research, Engineering and Technology (www.icrets.net) held in Budapest/Hungary on July 06-09 2023.

References

Azad, A. K., & Khan, M. M. K. (Eds.). (2021). *Bioenergy Resources and Technologies*. Academic Press.

Burton, N. A., Padilla, R. V, Rose, A., & Habibullah, H. (2020). Increasing the efficiency of hydrogen production from solar powered water electrolysis. *Renewable and Sustainable Energy Reviews*, *135*(08), 110255.

Esposito, D. V. (2017). Membraneless electrolyzers for low-cost hydrogen production in a renewable energy future. *Joule*, *1*(4), 651–658.

Gambou, F., Guilbert, D., Zasadzinski, M., Rafaralahy, H., Gambou, F., Guilbert, D., Zasadzinski, M., Rafaralahy, H., Gambou, F., Guilbert, D., Zasadzinski, M., & Rafaralahy, H. (2022). A comprehensive survey of alkaline electrolyzer modeling : electrical domain and specific electrolyte conductivity. *Energies*, *15*(9), 3452.

Gopinath, M., & Marimuthu, R. (2022). A review on solar energy-based indirect water-splitting methods for hydrogen generation. *International Journal of Hydrogen Energy*, *47*(09), 37742–37759.

Hofrichter, A., Rank, D., Heberl, M., & Sterner, M. (2022). Determination of the optimal power ratio between

electrolysis and renewable energy to investigate the effects on the hydrogen production costs. *International Journal of Hydrogen Energy*, *48(5)*, 1651-1663.

Islam, M. H., Lamb, J. J., Burheim, O. S., & Pollet, B. G. (2020). Ultrasound-assisted electrolytic hydrogen production. In *Micro-Optics and Energy: Sensors for Energy Devices* (pp. 73–84), Springer Nature

Kerboua, K., & Merabet, N. H. (2023). Sono-electrolysis performance based on indirect continuous sonication and membraneless alkaline electrolysis: Experiment, modelling and analysis. *Ultrasonics Sonochemistry*, *96*(2), 106429.

Li, S. De, Wang, C. C., & Chen, C. Y. (2009). Water electrolysis in the presence of an ultrasonic field. *Electrochimica Acta*, *54*(15), 3877–3883.

Marini, S., Salvi, P., Nelli, P., Pesenti, R., Villa, M., Berrettoni, M., Zangari, G., & Kiros, Y. (2012). Advanced alkaline water electrolysis. *Electrochimica Acta*, *82*(05), 384–391.

Maurer, W., Rechberger, P., Justl, M., & Keuschnigg, R. (2022). Parameter study for dimensioning of a PV optimized hydrogen supply plant. *International Journal of Hydrogen Energy*, *47*(10), 40815–40825.

Mohamed, B., Ali, B., Ahmed, B., Ahmed, B., Salah, L., & Rachid, D. (2016). Study of hydrogen production by solar energy as tool of storing and utilization renewable energy for the desert areas. *International Journal of Hydrogen Energy*, *41*(45), 20788–20806.

Merabet, N. M., & Kaouther Kerboua, O. H. (2023). Converting PV solar energy to green hydrogen. In *Reference Module in Earth Systems and Environmental Sciences* (pp. 1–10). Elsevier

Pang, X., Davis, J. T., & Esposito, D. V. (2020). Framework for evaluating the performance limits of membraneless electrolyzers. *Energy and Environmental Science*, *13*, 3663–3678.

Rahim, A. H. A., Salami, A., Fadhlullah, M., Hanapi, S., & Sainan, K. I. (2015). Optimization of direct coupling solar PV panel and advanced alkaline electrolyzer system. *Energy Procedia*, *79*, 204–211.

Tijani, A. S., Afiqah, N., & Kamarudin, B. (2018). Investigation of the effect of charge transfer coefficient (CTC) on the operating voltage of polymer electrolyte membrane (PEM) electrolyzer. *International Journal of Hydrogen Energy*, *43*(19), 9119-9132.

Villalva, M. G., Gazoli, J. R., & Filho, E. R. (2009). Comprehensive approach to modeling and simulation of photovoltaic arrays. *IEEE Transactıons On Power Electronıcs*, *24*(5), 1198–1208.

Walton, D. J., Burket, L. D., & Murphy, M. M. (1996). Sonoelectrochemistry :Clorine, hydrogen and oxygen evolution at platinised platinium. *Elecrrochimica ACta*, *41*(17), 2747–2751.

Zadeh, S. H. (2014). Hydrogen production via ultrasound-aided alkaline water electrolysis. *Automation and Control Engineering*, *2*(1), 103-109

Author Information

Nour Hane Merabet
Center of Applied Research, Karlsruhe University of Applied Sciences, Moltkestr, 30, 76133 Karlsruhe, Germany
National Higher School of Technology and Engineering, 23005 Annaba, Algeria
Laboratory of Technologies of Energetic Systems E3360100, 23005 Annaba, Algeria
Contact e-mail:n.merabet@esti-annaba.dz

Kaouther Kerboua
National Higher School of Technology and Engineering, 23005 Annaba, Algeria

To cite this article:

Merabet N. H. & Kerboua K. (2023), Green hydrogen from PV-supplied sono-electrolysis: Modelling and experimental investigations of the mechanism and performance. *The Eurasia Proceedings of Science, Technology, Engineering & Mathematics (EPSTEM), 23*, 100-105.